METRICA
METRology Institutional CAtalog

ISTITUTO NAZIONALE DI RICERCA METROLOGICA
Repository Istituzionale

Uncertainty propagation in field inversion for turbulence modelling in turbomachinery

This is the author's accepted version of the contribution published as:

Original
Uncertainty propagation in field inversion for turbulence modelling in turbomachinery / Ferrero, A., Larocca, F., Pennecchi, F.R.. - (2020), pp. 303-308. (2020 IEEE 7th International Workshop on Metrology for AeroSpace (MetroAeroSpace)) [10.1109/MetroAeroSpace48742.2020.9160187].

Availability:
This version is available at: 11696/66180 since: 2021-02-12T12:47:35Z

Publisher:

Published
DOI:10.1109/MetroAeroSpace48742.2020.9160187

Terms of use:

This article is made available under terms and conditions as specified in the corresponding bibliographic description in the repository

Publisher copyright
IEEE
© 20XX IEEE. Personal use of this material is permitted. Permission from IEEE must be obtained for all other uses, in any current or future media, including reprinting/republishing this material for advertising or promotional purposes, creating new collective works, for resale or redistribution to servers or lists, or reuse of any copyrighted component of this work in other works

(Article begins on next page)

13 October 2026

Uncertainty propagation in field inversion for turbulence modelling in turbomachinery

1st Andrea Ferrero
Department of Mechanical and Aerospace Engineering
Politecnico di Torino
Torino, Italy
andrea_ferrero@polito.it

2nd Francesco Larocca
Department of Mechanical and Aerospace Engineering
Politecnico di Torino
Torino, Italy
francesco.larocca@polito.it

3rd Francesca Romana Pennecchi
Applied Metrology and Engineering Division
Istituto Nazionale di Ricerca Metrologica
Torino, Italy
f.pennecchi@inrim.it

***Abstract*—The simulation of turbulent flows in turbomachinery requires to describe a wide range of scales and non-linear phenomena. Since the cost of scale resolving simulations is prohibitive for several configurations, turbulence closure models are still widely used in the framework of Reynolds-averaged Navier-Stokes (RANS) equations. In order to improve the prediction capability of these models, several machine learning strategies have been proposed. Among them, the field inversion approach allows to find a correction field which can be applied to the source term of the turbulence model in order to match experimental data: the correction field can then be generalised and expressed as a function of some flow features in order to extract modelling knowledge from the data.**

However, the reference experimental data are affected by uncertainty and this propagates to the correction field and to the final data-augmented model. In this work, the uncertainty propagation from the reference experimental data to the correction field is investigated. In particular, the flow field around a low pressure gas turbine cascade is studied in a challenging working condition characterised by laminar separation and transition to turbulence. The original RANS results are improved by the application of the field inversion algorithm in which the required gradients are computed by means of an adjoint approach. A sensitivity analysis is performed in order to provide a linearised propagation of the uncertainty from the experimental wall isentropic Mach number to the correction field.

***Index Terms*—turbulence model, turbomachinery, machine learning, uncertainty propagation, field inversion**

I. Introduction

The flow field in turbomachinery is characterised by strongly non-linear phenomena like shock waves, turbulence and separations. The recent grow in computational power has made it possible to perform scale resolving simulation for several turbomachinery flows. However, the computational cost of this kind of simulation (Direct Numerical Simulation or wall-resolved Large Eddy Simulation) is very high due to the large range of turbulence scales which characterise these flows and which is related to the relatively high Reynolds number of these configurations ($10^5 - 10^6$). Furthermore, scale resolving simulations can be performed for reduced domains with periodic boundary conditions but they become prohibitively expensive when full annulus multi-stage configurations are investigated. This is particularly true during the initial phases of the design process in which several different geometries should be investigated. A comprehensive review of high-fidelity simulation techniques for gas turbines was presented by [1].

In order to reduce the computational cost, Reynolds-averaged Navier-Stokes (RANS) equations are widely used for turbomachinery simulations. The idea behind this approach is to solve the average field by introducing a closure model for the unresolved scales. The price to pay in this kind of approaches is related to the errors which the model introduces in the description of several phenomena, in particular when separation or laminar to turbulence transition occurs.

While there are several research efforts related to the development of new turbulence closure models by means of physics-based theoretical considerations, some recent efforts have been devoted to the exploitation of the available experimental data by means of machine learning techniques. Among the different approaches, Parish and Duraisamy [2] proposed a strategy based on two steps: field inversion and machine learning. In the field inversion step, an optimisation problem is solved in order to find a correction field which allows to minimise the prediction error on a certain goal quantity. This correction field can be applied as a multiplier factor in the source term of the turbulence transport equation. This step requires the knowledge of high-fidelity reference data which can be obtained from experimental results or scale resolving simulations.

The second step based on machine learning allows to generalise the result to different working conditions and geometries with respect to the one used for field inversion: artificial neural networks can be used to identify a correlation between some physical quantities and the correction factor in order to improve the original closure model.

However, the quality of the obtained results will be strongly

related to the accuracy of the high-fidelity data used to drive the field inversion algorithm. In this work, the attention is focused on the sensitivity of the correction factor with respect to the experimental data. In particular, a perturbative approach is applied in order to estimate the sensitivity and understand how the uncertainty in the reference data propagates through the procedure. In the framework of the Guide to the expression of uncertainty in measurement (GUM) [3], the uncertainty associated with the input quantities of a measurement model is propagated by means of the Law of Propagation of Uncertainty (LPU), based on a linearization of the model itself. Other approaches are applicable, such as the propagation of probability distributions, modelling the input quantities, by means of Monte Carlo simulations [4], but they are not investigated in the present work.
The study is performed on the flow field in the T106c low pressure gas turbine cascade for aeronautical applications. The field inversion is based on the minimisation of the norm-2 error on the wall isentropic Mach number distribution with respect to the available experimental data.

II. Numerical framework

A. Turbulence closure

The compressible RANS equations with the Spalart-Allmaras (SA) turbulence closure [5] are considered in this work. The transport equations for the modified eddy viscosity $\hat{\nu}$ is:

$$\frac{\partial \rho\hat{\nu}}{\partial t} + \nabla\cdot(\rho\boldsymbol{u}\hat{\nu}) = \rho\left[\beta\tilde{P} - \tilde{D}\right] + \frac{1}{\sigma}\nabla\cdot(\rho(\nu+\hat{\nu})\nabla\hat{\nu}) + \\ + \frac{c_{b2}}{\sigma}\rho(\nabla\hat{\nu})^2 - \frac{1}{\sigma}(\nu+\hat{\nu})\nabla\rho\cdot\nabla\hat{\nu} \tag{1}$$

where ρ, $\boldsymbol{u}$, ν, $\hat{\nu}$, $\tilde{P}$ and $\tilde{D}$ are density, velocity, molecular viscosity, modified eddy viscosity, production and destruction terms, respectively. More details on the implementation and the values of the constants σ and c_{b2} can be found in [5]. The term β represents the correction field which is computed in the field inversion framework to improve the model.
The SA turbulence model is suitable for high Reynolds number flows with fully turbulent behaviour. However, it is applied in this work to the low Reynolds number flow around the T106c cascade. In particular, the exit isentropic Reynolds number is $8\cdot10^4$ and the exit isentropic Mach number is 0.65. The inlet turbulence level is set to $\tilde{\nu}/\nu = 0.1$, a very low value which is representative of the almost laminar conditions observed in the experiments. In these conditions the flow is characterised by laminar separation followed by transition: since the SA model is not suitable for describing these phenomena, the correction field $\beta(\boldsymbol{x})$ will act as an intermittency model, limiting the turbulence production in the first part of the cascade.

B. Numerical discretisation

The governing equations are integrated by means of the method of lines: the discontinuous Galerkin method is used for the spatial discretisation while time integration is performed by means of the implicit Euler scheme. The methods are implemented in a research code that has been verified and validated for turbulent and compressible flows [6]–[8].
The solution inside each element is described by an orthonormal and hierarchical modal basis implemented following the approach of [9]: a third order accurate reconstruction is adopted for this work. Convective and diffusive terms are evaluated by means of an approximate Riemann solver [10], [11] and a recovery-based method [12], respectively.
The implicit Euler scheme requires to solve a linear system at each time step: the GMRES algorithm with the additive Schwarz preconditioner is adopted in this work and the PetsC library [13] is employed to solve the system in a parallel MPI environment. The computational domain is dicretised by means of an unstructured mesh generated by the frontal Delaunary for quads algorithm [14] provided by the Gmsh tool [15]. The grid contains 40444 elements and it is reported in Figure 1. Since a third order accurate DG scheme is employed, six degrees of freedom are introduced inside each element: the total number of degrees of freedom per equation is 242664. This resolution level was chosen after a grid refinement analysis and allows to get grid independent results.

C. Field inversion

The field inversion algorithm requires to solve an optimisation problem in which the optimal field β is determined in order to minimise the following goal function G:

$$G = \int_w (M_s - M_s^{exp})^2 dl \tag{2}$$

The integral is the norm-2 error between the wall isentropic Mach number M_s distribution and the experimental value M_s^{exp} on the blade surface w. The procedure is initialised from a steady solution of the original SA model (i.e. $\beta(\boldsymbol{x}) = 1$). The gradient descent method is employed to find the solution of the optimisation problem, which is particularly expensive because the size of the parameter space corresponds to the number of degrees of freedom of the mesh (of the order of 10^5). In order to efficiently evaluate the gradient, the discrete adjoint method is adopted following the approach of [16]. The optimisation process requires to perform approximately 50 fully converged steady RANS simulations.
Fig. 2 shows the wall isentropic Mach number distribution for the original SA model, the optimised SA model and the experimental data. The results show the significant improvement that the field inversion approach can introduce: the plateau region which is observed in the experimental distribution is related to the separation region which is missing in the original SA results but is clearly visible in the simulation performed with the optimised model. This behaviour is confirmed by the Mach field comparison reported in Fig. 3 and 4, where the open separation can be clearly identified. The modified turbulent eddy viscosity $\tilde{\nu}$ normalised with respect to the kinematic viscosity ν is reported in Figure 5 and 6 for both the original model and the optimal solution, respectively. The

Figures show clearly that the open separation observed in the optimal solution leads to large values of eddy viscosity in the wake: this will strongly influence also the wake losses predicted by the simulation.
In Fig. 7 the optimal β field obtained by the field inversion process is reported. The results show that the correction field tends to deactivate the turbulence production in the first part of the boundary layer in order to achieve laminar behaviour in this region.

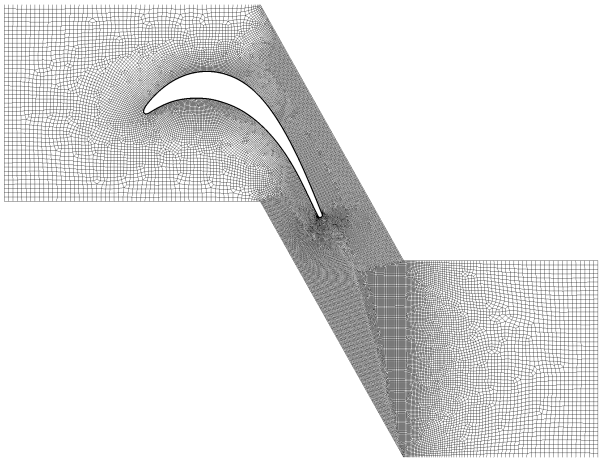

Fig. 1. Unstructured computational mesh with 40444 elements.

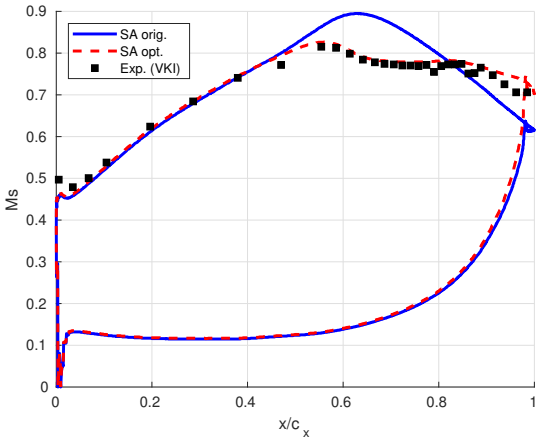

Fig. 2. Wall isentropic Mach number distribution for T106c cascade.

D. Machine learning from correction field

The correction field $\beta(\boldsymbol{x})$ is produced by the optimisation procedure and it is referred to the particular geometry and working condition which were considered in the reference experimental setup. This makes the correction $\beta(\boldsymbol{x})$ quite useless, since it cannot be applied to a general problem with different working conditions for which experimental data are missing. In order to exploit the correction term for actual predictions it is necessary to generalise the results and to express the correction field $\beta(\boldsymbol{\Phi})$ as a function of some

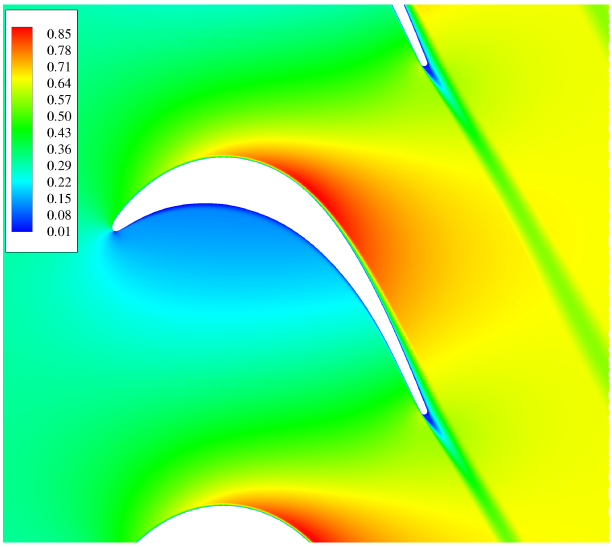

Fig. 3. Mach field with the original SA model.

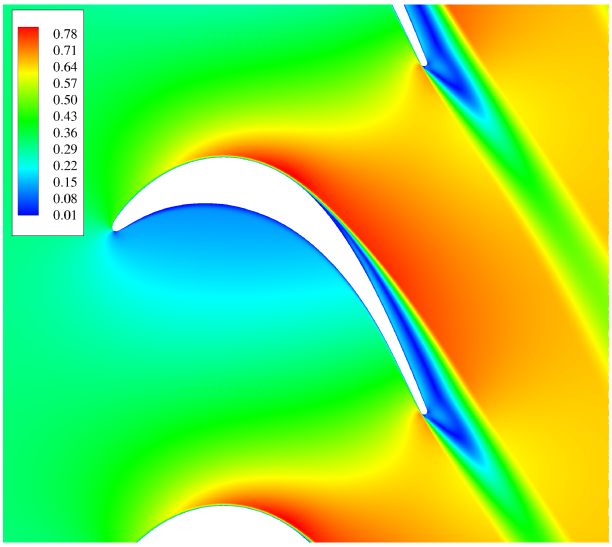

Fig. 4. Mach field with the optimised SA model obtained by field inversion.

flow features $\boldsymbol{\Phi}$: in this way a data-augmented RANS model is obtained. This can be done by analysing the database obtained by the field inversion procedure: for each mesh point, not just the correction factor β, but also all the flow properties are available. In this way, it is possible to identify some features (non-dimensional variables which satisfy Galileian invariance) which can be used as inputs for the computation of β. The correlation between the features $\boldsymbol{\Phi}$ and β can be identified following several approaches. Parish and Duraisamy [2] proposed the use of artificial neural networks for this purpose. It is possible to enrich the training database by performing the inversion procedure for several working conditions and then joining the databases in order to explore a larger range of input variables and increase the predictive capability of the final data-augmented model. An application

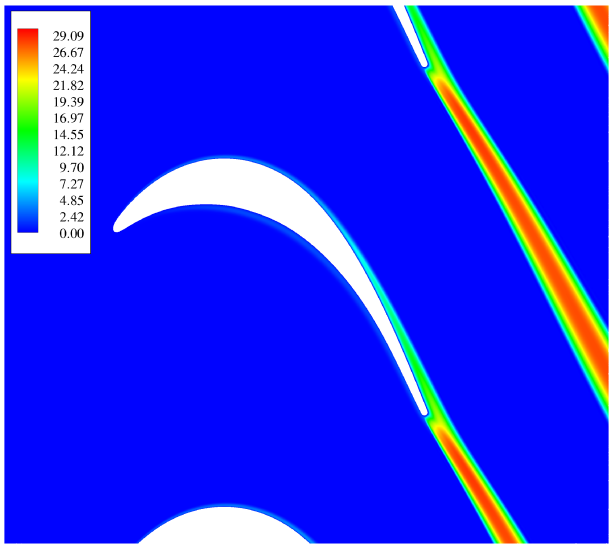

Fig. 5. Normalised turbulent eddy viscosity $\tilde{\nu}/\nu$ field with the original SA model.

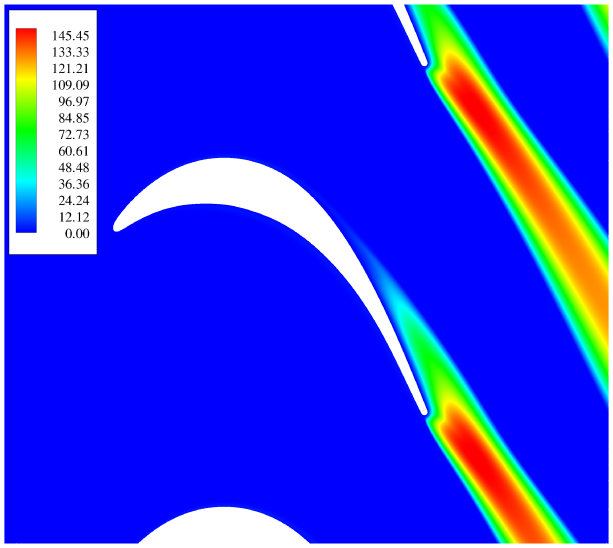

Fig. 6. Normalised turbulent eddy viscosity $\tilde{\nu}/\nu$ field with the optimised SA model.

of this approach to turbomachinery flows was investigated by Ferrero et al. [17]. In the present work the machine learning analysis is not discussed. The key point investigated here is related to the fact that the reference experimental data are affected by a measurement uncertainty and so, as a consequence, also the correction field provided by the field inversion procedure is. It is important to quantify the β uncertainty because the correction field is computed with the purpose of building a new model through the machine learning analysis. However, the model obtained by machine learning will reproduce the pattern observed in the database: for this reason, the measurement uncertainty in the original reference data propagates through the numerical procedures and contributes to the modelling uncertainty associated to the

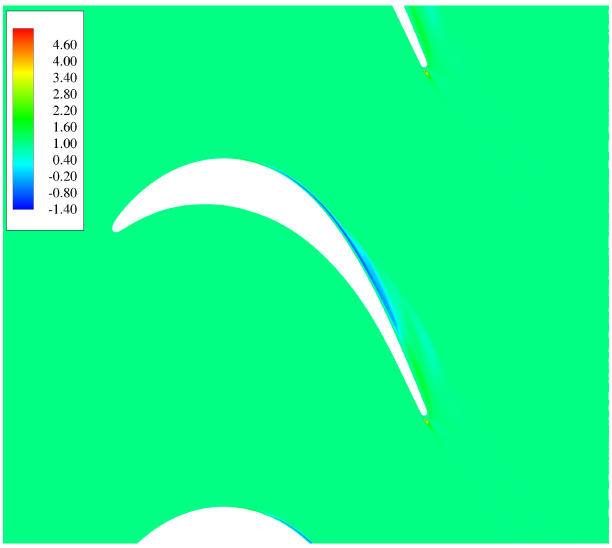

Fig. 7. Optimal β field obtained by field inversion.

final data-augmented RANS model.

III. Uncertainty propagation

The correction $\beta(\boldsymbol{x})$ is computed by the field inversion procedure in order to match the predicted wall isentropic Mach number distribution with the experimental data. The goal of this work is to estimate the sensitivity of the field $\beta(\boldsymbol{x})$ with respect to the experimental data. This is done by propagating the uncertainty in the experimental data through the linearization of the considered model, which consists in the minimization of the goal function (2). Since this is an implicit model for which analytical derivatives are hard to derive, a numerical approximation of the uncertainty associated with $\beta(\boldsymbol{x})$ is obtained by introducing a fixed relative perturbation ϵ_{rel} in the experimental data and calculating which is the corresponding effect in the output with respect to the unperturbed input:

$$M_s^{exp\pm}(x) = M_s^{exp}(x)(1 \pm \epsilon_{\text{rel}}) \ , \tag{3}$$

where $\epsilon_{\text{rel}} = 1\,\%$ was used. This value was suggested by the relative uncertainty associated to the experimental Mach number which typically ranged between $0.4\,\% - 1.2\,\%$ according to [18].

The uncertainty field $u(\boldsymbol{x})$ is numerically evaluated according to:

$$u(\boldsymbol{x}) = \frac{\left|\beta(\boldsymbol{x})|_{M_s^{exp+}} - \beta(\boldsymbol{x})|_{M_s^{exp-}}\right|}{2}. \tag{4}$$

A similar kind of approximation is suggested in [3, sec. 5.1.3, NOTE 2], where each input quantity at a time is made varying by its relevant uncertainty and then the corresponding numerical differences in the output are summed up in quadrature, hence providing a combined standard uncertainty for the measurand. In the present case study, however, the perturbation of each input quantity at a time and the evaluation

of the corresponding model would be extremely heavy from a computational point of view. Therefore, in expression (4), it was decided to perturbe all the input quantities simultaneously, each with respect to its relative uncertainty, hence model $\beta(\boldsymbol{x})|_{M_s^{exp\pm}}$ could be evaluated just once. It can be seen that such a procedure leads to an overevaluation of the combined standard uncertainty for the measurand, so that it is prudentially conservative.

In Fig. 8 the $u(\boldsymbol{x})$ field is reported showing that a significant uncertainty is observed in correspondence of some regions of the separated shear layer, close to the trailing edge and in a portion of the boundary layer on the suction side.

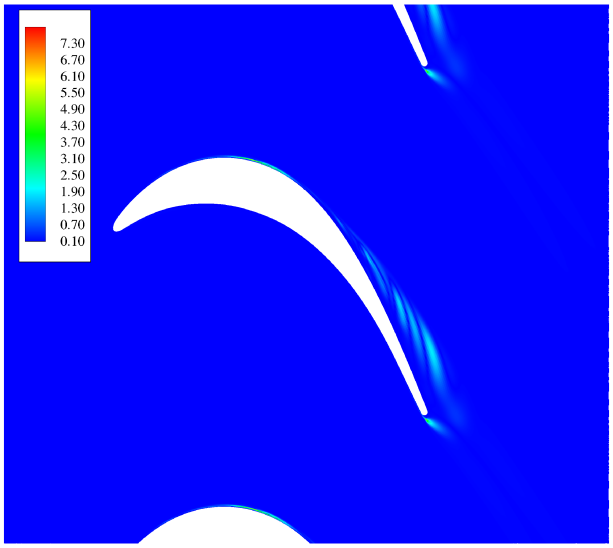

Fig. 8. Uncertainty on the correction field β.

IV. Conclusions

The field inversion approach represents a promising strategy to generate correction fields which can be exploited by machine learning techniques to improve existing RANS models. However, particular care should be devoted to the definition of the reference quantities which are used to drive the field inversion procedure. In the present study, the experimental uncertainty on the wall isentropic Mach number distribution on a low pressure gas turbine cascade is considered and propagated to the correction field: the preliminary analysis shows that in some regions of the domain there is a significant amplification of the relative uncertainty between the input data and the obtained correction field. This suggests that the correction factor in these region should be carefully considered during the training of the data-augmented RANS model: a possible solution could be related to the use of local weights which reduce the relative importance of data points which are characterised by large uncertainties. Furthermore, the goal function used in this work for the field inversion procedure contains only the error on the wall isentropic Mach number distribution. It is possible to augment the goal function by adding a Tikhonov regularisation [19] which penalises the correction factor when it assumes values far from unity [16]: in this way the correction is introduced only where it gives a significant improvement in the goal functions and unnecessary high correction factors with limited benefits are avoided. This regularisation could reduce the sensitivity of the correction field to the reference data and so it could limit the uncertainty on the data-augmented RANS model.

Acknowledgment

Computational resources were provided by HPC@POLITO, a project of Academic Computing within the Department of Control and Computer Engineering at the Politecnico di Torino (http://www.hpc.polito.it). We acknowledge the CINECA award under the ISCRA initiative, for the availability of high performance computing resources and support. The simulations were performed on the Marconi Tier-0 System for the Project FIRST.

References

[1] R. D. Sandberg and V. Michelassi, "The current state of high-fidelity simulations for main gas path turbomachinery components and their industrial impact," *Flow, Turbulence and Combustion*, vol. 102, no. 4, pp. 797–848, 2019.

[2] E. J. Parish and K. Duraisamy, "A paradigm for data-driven predictive modeling using field inversion and machine learning," *Journal of Computational Physics*, vol. 305, pp. 758–774, 2016.

[3] BIPM, IEC, IFCC, ILAC, ISO, IUPAC, IUPAP, and OIML, *Guide to the Expression of Uncertainty in Measurement, JCGM 100:2008, GUM 1995 with minor corrections*. BIPM, 2008.

[4] *BIPM, IEC, IFCC, ILAC, ISO, IUPAC, IUPAP and OIML, Supplement 1 to the 'Guide to the Expression of Uncertainty in Measurement' – Propagation of distributions using a Monte Carlo method, JCGM 101:2008*. BIPM, 2008.

[5] S. R. Allmaras and F. T. Johnson, "Modifications and clarifications for the implementation of the Spalart-Allmaras turbulence model," in *Seventh international conference on computational fluid dynamics (ICCFD7)*, 2012, pp. 1–11.

[6] A. Ferrero and F. Larocca, "Feedback filtering in discontinuous Galerkin methods for Euler equations," *Progress in Computational Fluid Dynamics, an International Journal*, vol. 16, no. 1, pp. 14–25, 2016.

[7] E. Ampellio, F. Bertini, A. Ferrero, F. Larocca, and L. Vassio, "Turbomachinery design by a swarm-based optimization method coupled with a CFD solver," *Advances in aircraft and spacecraft science*, vol. 3, no. 2, p. 149, 2016.

[8] A. Ferrero and F. Larocca, "Adaptive CFD schemes for aerospace propulsion," in *Journal of Physics: Conference Series*, vol. 841, no. 1. IOP Publishing, 2017, p. 012017.

[9] F. Bassi, L. Botti, A. Colombo, D. A. Di Pietro, and P. Tesini, "On the flexibility of agglomeration based physical space discontinuous Galerkin discretizations," *Journal of Computational Physics*, vol. 231, no. 1, pp. 45–65, 2012.

[10] S. Osher and F. Solomon, "Upwind difference schemes for hyperbolic systems of conservation laws," *Mathematics of computation*, vol. 38, no. 158, pp. 339–374, 1982.

[11] M. Pandolfi, "A contribution to the numerical prediction of unsteady flows," *AIAA journal*, vol. 22, no. 5, pp. 602–610, 1984.

[12] A. Ferrero, F. Larocca, and G. Puppo, "A robust and adaptive recovery-based discontinuous Galerkin method for the numerical solution of convection–diffusion equations," *International Journal for Numerical Methods in Fluids*, vol. 77, no. 2, pp. 63–91, 2015.

[13] S. Balay, S. Abhyankar, M. Adams, J. Brown, P. Brune, K. Buschelman, L. Dalcin, A. Dener, V. Eijkhout, W. Gropp *et al.*, "PETSc users manual," 2019.

[14] J.-F. Remacle, F. Henrotte, T. Carrier-Baudouin, E. Béchet, E. Marchandise, C. Geuzaine, and T. Mouton, "A frontal Delaunay quad mesh generator using the L∞ norm," *International Journal for Numerical Methods in Engineering*, vol. 94, no. 5, pp. 494–512, 2013.

[15] C. Geuzaine and J.-F. Remacle, "Gmsh: A 3-D finite element mesh generator with built-in pre-and post-processing facilities," *International journal for numerical methods in engineering*, vol. 79, no. 11, pp. 1309–1331, 2009.

[16] A. P. Singh, S. Medida, and K. Duraisamy, "Machine-learning-augmented predictive modeling of turbulent separated flows over airfoils," *AIAA Journal*, pp. 2215–2227, 2017.

[17] A. Ferrero, A. Iollo, and F. Larocca, "Field inversion for data-augmented RANS modelling in turbomachinery flows," *Computers & Fluids*, vol. 201, p. 104474, 2020.

[18] J. Michalek, M. Monaldi, and T. Arts, "Aerodynamic performance of a very high lift low pressure turbine airfoil (T106C) at low Reynolds and high Mach number with effect of free stream turbulence intensity," *Journal of Turbomachinery*, vol. 134, no. 6, p. 061009, 2012.

[19] C. M. Bishop, "Training with noise is equivalent to Tikhonov regularization," *Neural computation*, vol. 7, no. 1, pp. 108–116, 1995.